JVI Journals.ASM.org

Signal Transducer and Activator of Transcription 3 Limits Epstein-Barr Virus Lytic Activation in B Lymphocytes

Erik R. Hill,[a]* Siva Koganti,[a] Jizu Zhi,[b] Cynthia Megyola,[c] Alexandra F. Freeman,[d] Umaimainthan Palendira,[e] Stuart G. Tangye,[e] Paul J. Farrell,[f] Sumita Bhaduri-McIntosh[a,g]

Division of Infectious Diseases, Department of Pediatrics and Stony Brook Children's Hospital, Stony Brook University, Stony Brook, New York, USA[a]; Bioinformatics Core Facility, Stony Brook University School of Medicine, Stony Brook, New York, USA[b]; Department of Genetics, Yale University School of Medicine, New Haven, Connecticut, USA[c]; Immunopathogenesis Section, Laboratory of Clinical Infectious Diseases, National Institutes of Health, Bethesda, Maryland, USA[d]; Immunology Program, Garvan Institute of Medical Research, Darlinghurst, NSW, Australia, and St. Vincent's Clinical School, University of NSW, Sydney, NSW, Australia[e]; Section of Virology, Imperial College Faculty of Medicine, St. Mary's Campus, London, United Kingdom[f]; Department of Molecular Genetics and Microbiology, Stony Brook University, Stony Brook, New York, USA[g]

Lytic activation of Epstein-Barr virus (EBV) is central to its life cycle and to most EBV-related diseases. However, not every EBV-infected B cell is susceptible to lytic activation. This lack of uniform susceptibility to lytic activation also directly impacts the success of viral oncolytic therapy for EBV cancers, yet determinants of susceptibility to lytic induction signals are not well understood. To determine if host factors influence susceptibility to EBV lytic activation, we developed a technique to separate lytic from refractory cells and reported that EBV lytic activation occurs preferentially in cells with lower levels of signal transducer and activator of transcription 3 (STAT3). Using this tool to detect single cells, we now extend the correlation between STAT3 and lytic versus refractory states to EBV-infected circulating B cells in patients with primary EBV infection, leading us to investigate whether STAT3 controls susceptibility to EBV lytic activation. In loss-of-function and gain-of-function studies in EBV-positive B lymphoma and lymphoblastoid cells, we found that the levels of functional STAT3 regulate susceptibility to EBV lytic activation. This prompted us to identify a pool of candidate cellular genes that might be regulated by STAT3 to limit EBV lytic activation. From this pool, we confirmed increases in transcript levels in refractory cells of a set of genes known to participate in transcription repression. Taken together, our findings place STAT3 at a critical crossroads between EBV latency and lytic activation, processes fundamental to EBV lymphomagenesis.

Epstein-Barr virus (EBV) infects most humans and persists silently in B lymphocytes. Primary infection with EBV can cause infectious mononucleosis (IM). Under certain circumstances, EBV can cause B-cell lymphomas and epithelial cell cancers (1). Several studies suggest that EBV lytic activation is an important step in the pathogenesis of such EBV-related diseases (2–5). From a therapeutic standpoint, efforts to eliminate EBV-positive tumors using nucleoside analogues after induction of viral lytic activation have shown promise (6–8). However, EBV-infected tumor cells are not fully permissive to lytic induction, as only a fraction of EBV-infected B cells exposed to lytic cycle-inducing agents enters the lytic cycle; the remainder of the population is refractory to lytic induction (9, 10). These refractory cells are not susceptible to oncolytic therapy, necessitating further investigations into the physiology underlying both lytic and refractory states.

A general problem with investigating EBV lytic activation is that a mixed population of refractory and lytic cells results from exposure to lytic cycle-inducing stimuli. We therefore developed a technique to separate lytic cells from refractory cells in a mixed population of EBV-infected B cells (9). Our previous studies using this technique showed that host cell determinants regulate susceptibility of EBV-infected B cells to lytic cycle-inducing stimuli (9, 11) and that higher levels of signal transducer and activator of transcription 3 (STAT3) in Burkitt lymphoma (BL) cells correlate with resistance to EBV lytic activation (11). Conversely, lower levels of STAT3 correlate with susceptibility to lytic activation. STAT3 drives prosurvival and proproliferative functions (12, 13) and is overactive in most human cancers (14). To exploit the EBV lytic program to drive oncolysis of EBV-infected tumors, the interplay between host molecules, such as STAT3, and EBV lytic activation needs to be understood.

We now demonstrate that during primary EBV infection, the majority of B lymphocytes detectable by antibodies against EBV lytic proteins have low STAT3 levels. We also show that STAT3 reduces susceptibility to lytic activation, thereby functionally linking STAT3 to lytic activation. As STAT3 can transcriptionally regulate thousands of genes, we used two genome-wide analyses to limit the data set of candidate transcriptional targets that may be modulated by STAT3 to curb EBV lytic activation. We expect this powerful resource to significantly accelerate efforts to map molecular mechanisms that underlie susceptibility of cells to EBV lytic activation.

Received 28 June 2013 **Accepted** 8 August 2013

Published ahead of print 21 August 2013

Address correspondence to Sumita Bhaduri-McIntosh, sumita.bhaduri-mcintosh@stonybrookmedicine.edu.

* Present address: Erik R. Hill, Department of Public Health, Campbell University College of Pharmacy and Health Sciences, Buies Creek, North Carolina, USA.

E.R.H. and S.K. contributed equally to this article.

Supplemental material for this article may be found at http://dx.doi.org/10.1128/JVI.01762-13.

doi:10.1128/JVI.01762-13

MATERIALS AND METHODS

Patients and cell lines. Blood was drawn from subjects after informed consent was obtained. The study of human subjects was approved by institutional review boards (IRBs) at Stony Brook University, the NIAID, and the Garvan Institute. IM patients, 8 and 14 years of age, had presented with 5 to 7 days of low-grade fever, sore throat, malaise, and headache. Serologies were consistent with primary EBV infection (presence of IgM and IgG to viral capsid antigen [VCA] but absence of IgG to EBNA). Peripheral blood mononuclear cells (PBMC) were isolated (15), and EBV-positive lymphoblastoid cell lines (EBV-LCL) from 10 healthy subjects and 10 patients with autosomal dominant hyper-IgE syndrome (AD-HIES) were generated according to protocols reported previously (15, 16). Five AD-HIES patients are monitored at the Garvan Institute (patient 4, described previously by Ma et al. [17], and patients 6, 7, 8, and 10, described previously by Avery et al. [16]), and five more are monitored at the NIAID (patients J002, J022, J098, and J100, described by Holland et al. [18]; J002 includes a parent-child pair). Three additional AD-HIES patients (patient J020, reported previously by Holland et al. [18], and two previously unreported patients) were used for the experiment shown in Fig. 3G. Six AD-HIES patients had a mutation in the SH2 domain, six had a mutation in the DNA-binding domain, and one had a mutation in the transactivation domain of *STAT3*. The EBV-infected HH514-16 cell line is a subclone of the P3J-HR1 BL cell line (19).

Chemical treatment of cell lines. HH514-16 cells were subcultured at 3×10^5 cells/ml; 48 h later, cells were treated with 3 mM sodium butyrate (NaB; Sigma), 5 μM 5-aza-2-deoxycytidine (Aza; Sigma), 25 μM AG490 (Cayman), and/or 5 μM WP1066 (Calbiochem). For EBV-LCL experiments, cells were grown at 1×10^6 cells/ml for 48 h and then subcultured at 3×10^5 cells/ml in 10% spent medium for 36 h in the presence of 25 μM AG490 or 10 μM Stattic (20).

Transfection of cell lines. HH514-16 cells were subcultured at 5×10^5 cells/ml 24 h prior to transfection, washed twice with phosphate-buffered saline (PBS), and incubated with 1 μg of plasmid DNA (pCMV-*STAT3* or pCMV-Neo; gifts from Nancy Reich) or 100 μM small interfering RNA (siRNA) (against *STAT3* or scrambled; Santa Cruz) per 1×10^6 cells in 100 μl of electroporation solution (Ingenio electroporation solution, catalog number MIR 50117; Mirus Bio). Cells were electroporated by using Amaxa Nucleofector II (U015 program) and then diluted to 3×10^5 cells/ml in complete RPMI medium. Cells were washed twice at 24 h posttransfection and then treated with 3 mM NaB. Cells were harvested at 72 h posttransfection (48 h post-NaB treatment). Transfection efficiency ranged between 10 and 15% of live cells.

Immunodetection. (i) Immunoblotting. Total cell extracts were electrophoresed in 10% SDS-polyacrylamide gels, transferred onto nitrocellulose membranes, and blocked by using 5% bovine serum albumin (BSA). Mouse monoclonal antibodies (Ab) were used to detect EBV early antigen-diffuse (EA-D) (R3 at a 1/1,000 dilution; Millipore), EBV ZEBRA (BZ1 at a 1/500 dilution; Santa Cruz), and β-actin (AC-15 at a 1/3,000 dilution; Sigma). Human EBV-seropositive reference serum was used to detect EBV small viral capsid antigen (sVCA).

(ii) Flow cytometry. For IM PBMC, cells were stained in PBS containing 5% fetal bovine serum (FBS) with allophycocyanin (APC)-conjugated anti-CD2 Ab (1/50 dilution; BD Pharmingen) or mouse IgG-APC (BD) control Ab and human EBV reference sera (positive or negative) followed by phycoerythrin (PE)-conjugated anti-human IgG (1/200 dilution; BD). Cells were fixed and permeabilized by using Cytofix/Cytoperm (BD) and incubated with anti-STAT3 Ab (C20 at a 1/50 dilution; Santa Cruz) followed by fluorescein isothiocyanate (FITC)-conjugated anti-rabbit IgG (1/200 dilution; Life Technologies). Lack of CD2 expression was used to enrich for B cells, as antibody binding to the B-cell marker CD19 or CD20 resulted in disintegration of lytically infected B cells. To detect lytic HH514-6 cells and LCL, anti-EA-D (R3 at a 1/100 dilution), anti-gp350 (72A1 at a 1/25 dilution; Millipore) (followed by FITC-conjugated anti-mouse Ab at a 1/200 dilution), or reference sera from healthy subjects were used after fixation/permeabilization. Bound human anti-lytic IgG and STAT3 Ab were detected by using FITC-conjugated anti-human Fab (1/200 dilution; Sigma) and Alexa 647-conjugated anti-rabbit IgG (1/500 dilution; Life Technologies), respectively. Specific binding by C20 was detected over background binding of rabbit IgG. EA-D-positive (EA-D$^+$) and gp350-positive cells were identified after comparison to isotype-control-labeled cells. Specific detection of lytic antigens by reference EBV-positive serum was determined over background detection of similarly treated cells by reference EBV-negative serum (with 0.5 to 1% detection as the cutoff) by using dot plot analyses (9, 11). All lymphocytes shown in Fig. 1 expressed STAT3, as determined by comparison to cells stained with rabbit IgG. Cells were further divided into STAT3^{hi} and STAT3^{lo} subpopulations after comparison with the level of expression of STAT3 in T cells. Events (100,000) were acquired by using a FACSCalibur instrument (BD), and data were analyzed by using FlowJo software (Tree Star). Statistical analysis was performed by using Prism v3.0 (GraphPad) and Excel 2010 (Microsoft).

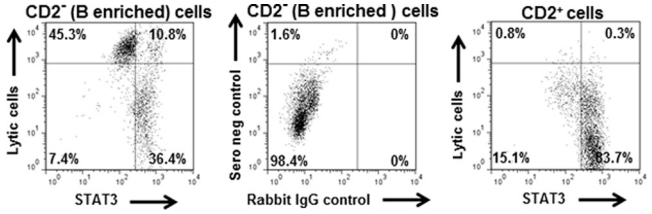

FIG 1 Lower levels of STAT3 mark peripheral blood B lymphocytes detected by antibodies to EBV lytic antigens. PBMC from a representative IM patient ($n = 2$) were surface stained with anti-CD2 Ab to distinguish between CD2$^+$ T and NK cells and CD2$^-$ non-T and non-NK cells (enriched for B cells). Cells were also surface stained with reference human sera followed by FITC-conjugated secondary Ab and anti-STAT3 Ab. CD2$^-$ cells (left) or CD2$^+$ cells (right) stained with EBV-positive reference serum and anti-STAT3 Ab are shown. The middle panel shows CD2$^-$ cells stained with EBV-negative reference serum and rabbit IgG (control for STAT3 Ab). Note that all lymphocytes expressed STAT3, as determined by comparison to cells stained with rabbit IgG. Cells were further divided into STAT3^{hi} and STAT3^{lo} subpopulations (designated by the line intersecting the *x* axis) after comparison with the level of expression of STAT3 in T cells.

Quantitative reverse transcription-PCR (qRT-PCR). Total RNA was isolated from EBV-LCL and HH514-16 cells by using an RNeasy kit (Qiagen) followed by DNase digestion (Promega). RNA was quantitated by using a NanoDrop instrument (Thermo Scientific). RNA (500 ng) was converted to cDNA by using qScript cDNA SuperMix (Quanta BioSciences). Relative transcript levels of selected cellular genes were determined with gene-specific primers by using Fast SYBR green Master Mix on a StepOne Plus thermocycler (Applied Biosystems). Sequences of primers for 18S and *STAT3* (11), *BMRF1* (21), and *BFRF3* (22) were reported previously. Sequences of other primers are as follows: SAFB forward primer GTTTTCCTCCAGCCCGTTAT and reverse primer TACC TCCGAGGGAAACAAGA, KEAP1 forward primer AAGAACTCCTCTT GCTTGGC and reverse primer CCAACTTCGCTGAGCAGATT, TFEB forward primer CTCCCGCTGCTCCTCCT and reverse primer CGGCA GTGCCTGGTACAT, ZFY forward primer CATCTTCATCCATGGC CTTT and reverse primer GTCGACACCACTGCGGAC, ZNF589 forward primer TCCAAATCCTCCTAACCCCT and reverse primer CTCT GCCTGCCAAGGATTC, SETDB1 forward primer TTCACGGAGCTTC TGGTCTT and reverse primer TTCCCGGCCTACAGAAATAA, LYL1 forward primer CTGCCTTCTCAGTCATGGTG and reverse primer AC CAGGCTGCAAGAACAGTG, ZNF557 forward primer GCTCCAGCTG GGAGATCAG and reverse primer TGTACAGGGACGTGATGCTG, and ZNF253 forward primer GGTCTTGGGCAAAATGAGAA and reverse primer CCTGGTTACCTGTCTGGAGC.

Relative expression levels were calculated by using the $\Delta\Delta C_T$ method, normalized to 18S rRNA levels, and compared to levels in untreated or vehicle-treated cells with StepOne software v2.2. Individual samples were

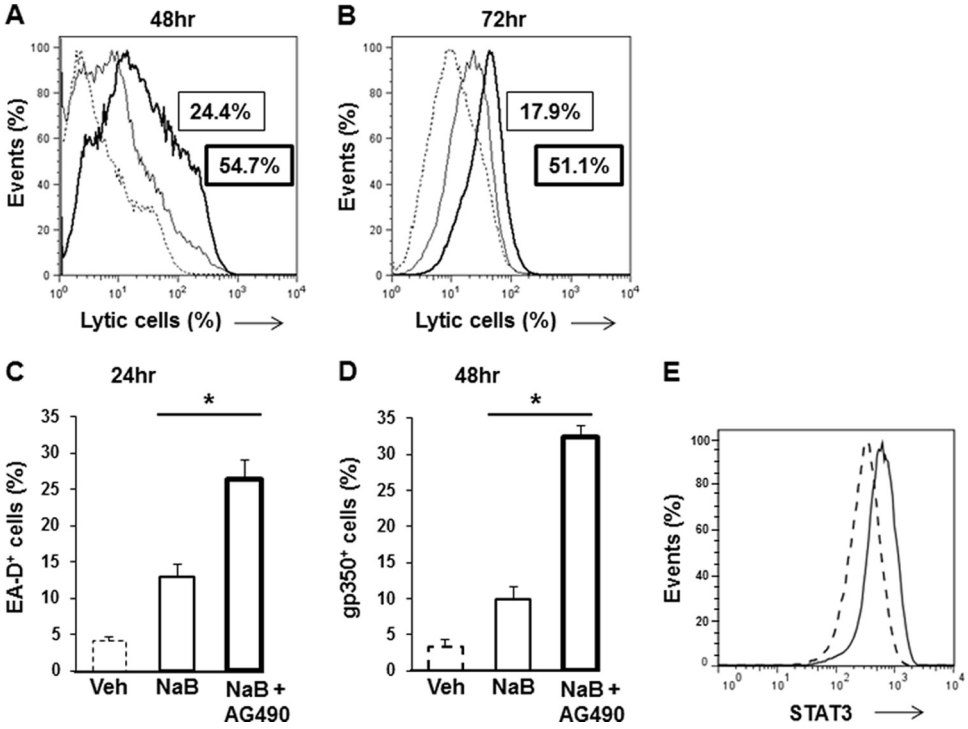

FIG 2 Lytic susceptibility of Burkitt lymphoma cells to known lytic cycle-inducing agents increases in the presence of AG490. (A and B) HH514-16 cells were treated for 48 h with NaB (A) or for 72 h with Aza (B) with or without AG490. Lytically infected cells were detected using reference human sera by flow cytometry (dotted line, vehicle-treated cells; solid line, NaB- or Aza-treated cells; bold line, NaB/Aza- and AG490-treated cells). Numbers in solid boxes represent the percentage of lytic cells in NaB- or Aza-treated cells compared to vehicle-treated cells; numbers in bold boxes represent the percentage of lytic cells in NaB/Aza- and AG490-treated cells compared to vehicle-treated cells. (C and D) Flow cytometric enumeration of cells expressing EA-D, an early lytic protein (C), or gp350, a late lytic protein (D), using specific MAbs following treatment of cells with NaB with or without AG490 for 24 or 48 h. (E) Intracellular levels of STAT3 in cells grown in the presence of vehicle (solid line) or AG490 (dashed line) for 48 h. Experiments were performed three times; error bars represent standard errors of the means. *, $P < 0.05$ by one-way analysis of variance with *post hoc* Bonferroni analysis.

assayed in triplicate. Statistical analysis was performed by using Prism v3.0 and Excel 2010.

RESULTS

Low levels of STAT3 mark *in vivo* B cells detected by antibodies to EBV lytic antigens. Transcriptome analysis of separated lytic and refractory cells led us to discover that lower levels of STAT3 correlate with lytic activation in EBV-positive BL cells (11). We asked whether this relationship between EBV and STAT3 also extends to EBV lytic activation *in vivo*. To do so, we needed to identify IM patients in very early stages of disease, ideally before the elimination of lytic B cells from the circulation by emerging T-cell responses. To correlate STAT3 levels and lytic gene expression in single cells, we used previously validated reference sera from EBV-positive subjects (or sera from EBV-naive subjects as a control) as a source of high-titer IgG to EBV lytic antigens (9, 11, 23). In contrast to the sensitive detection of cells supporting the EBV lytic cycle, we have demonstrated that these sera detect minimal to no latently infected cells in this assay (9). PBMC from two IM patients with very early disease were subjected to surface staining with reference human sera. Negative selection was used to enrich for B cells to avoid inadvertent activation of the EBV lytic cycle in B cells identified by antibodies to B-cell surface markers. We found that 54.5% (45.3% + 10.8% − 1.6% [representative data]) (Fig. 1) of $CD2^-$ (i.e., B-cell-enriched) cells were detected by reference EBV-positive serum. Of the $CD2^-$ cells, 47.2% expressed high levels of STAT3. Of the $STAT3^{hi}$ cells, 77.1% were nonlytic, while 86% of $STAT3^{lo}$ cells were lytic, demonstrating an enrichment of lytic cells among the $STAT3^{lo}$ population. In comparison, nearly all $CD2^+$ T and NK cells lacked staining for lytic antigens. Thus, lytically infected B cells are detectable in peripheral blood during IM, and lower levels of STAT3 correlate with EBV lytic activation *in vivo*.

Pharmacologic inhibition of STAT3 function enhances susceptibility to known lytic stimuli. To determine whether the intracellular level of STAT3 influences susceptibility to lytic activation, we used AG490, which inhibits phosphorylation/activation of STAT3 by Janus kinases (24). This inhibition in turn results in lower levels of total STAT3, as phosphorylated STAT3 drives the transcription of *STAT3* (25). HH514-16 BL cells were exposed to sodium butyrate (NaB) or 5-azacytidine (Aza), two agents that induce lytic activation by different mechanisms (26), in the presence or absence of AG490. Using reference human sera to identify cells expressing EBV lytic antigens (9, 11), we found that the addition of AG490 resulted in greater fractions of cells undergoing lytic activation by NaB or Aza than those treated with inducing agents alone (Fig. 2A and B). In separate experiments, we used monoclonal antibodies to early (EA-D) and late (gp350) lytic EBV antigens (Fig. 2C and D) to identify lytically infected cells. The addition of AG490 resulted in a >2-fold increase in the fraction of EA-D-positive cells over NaB treatment alone (Fig. 2C) when cells

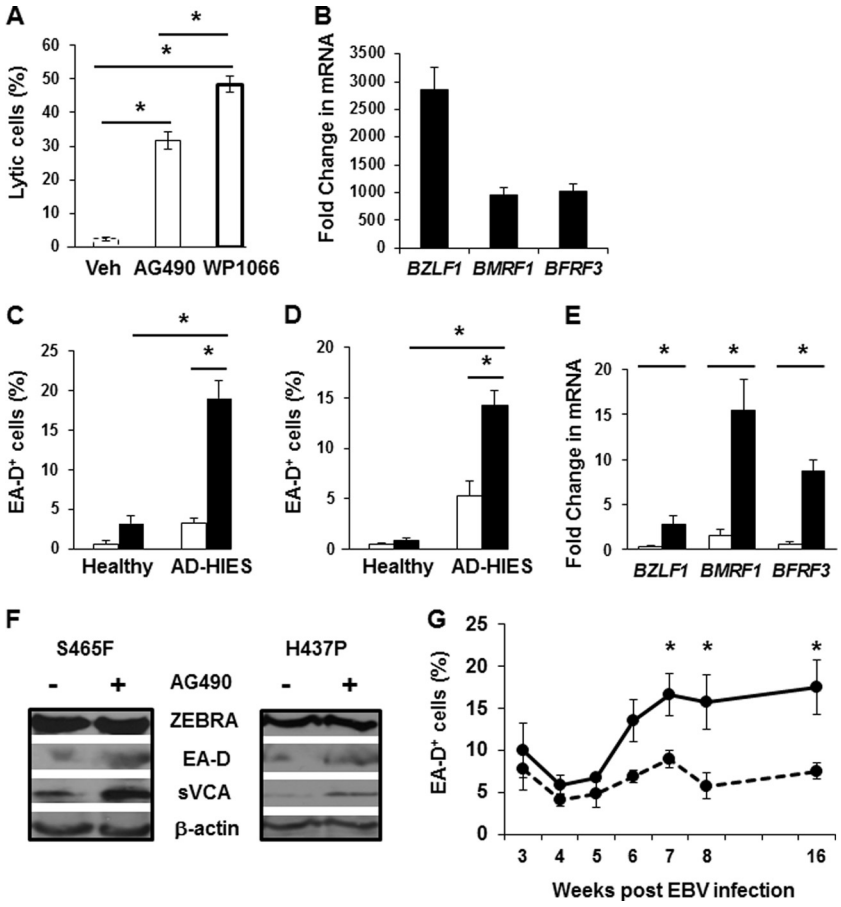

FIG 3 Inhibition of STAT3 function is sufficient to induce EBV lytic activation. (A) HH514-16 cells were treated with AG490 or WP1066, followed by staining with reference human sera and flow cytometric enumeration of lytically infected cells at 48 h. Vehicle-treated (dashed line), AG490-treated (solid line), and WP1066-treated (bold line) cells are indicated. Means from three experiments are shown; error bars indicate standard errors of the means. (B) qRT-PCR detection of EBV lytic gene transcripts (immediate early transcript *BZLF1*, early transcript *BMRF1*, and late transcript *BFRF3*) in cells treated for 48 h with vehicle or WP1066. The fold changes in mRNA levels in WP1066-treated over vehicle-treated cells after normalization to 18S rRNA levels using the $\Delta\Delta C_T$ method are shown. Experiments were performed three times, and means ± standard errors of the means are shown. (C and D) Flow cytometric enumeration of the percentage of EA-D$^+$ cells following treatment of healthy donor-derived LCL and AD-HIES patient-derived LCL with vehicle (open bars), AG490 (filled bars) (36-h treatment; $n = 10$ each for healthy and AD-HIES-derived LCL) (C), or Stattic (filled bars) (1-h treatment; $n = 5$ each for healthy and AD-HIES-derived LCL) (D). (E) qRT-PCR detection of EBV lytic gene transcripts in healthy donor-derived LCL (open bars) ($n = 3$) and AD-HIES-derived LCL (filled bars) ($n = 5$) treated with AG490. The fold changes in mRNA levels in the presence of AG490 over vehicle treatment for 36 h after normalization to 18S rRNA levels using the $\Delta\Delta C_T$ method are shown. (F) Immunoblot analysis of the EBV lytic proteins ZEBRA, EA-D, and sVCA in AD-HIES-derived LCL (*STAT3* mutations S465F and H437P) treated for 36 h with vehicle or AG490. (G) Spontaneous lytic activation in LCL detected by intracellular staining for EA-D by flow cytometry at different times post-EBV infection (dashed line, healthy donor-derived LCL; solid line, AD-HIES-derived LCL [$n = 3$ for each type]). In all panels, means ± standard errors of the means are indicated. *, $P < 0.05$ by one-way analysis of variance with *post hoc* Bonferroni analysis.

were harvested at 24 h. At 48 h, NaB plus AG490 resulted in a >3-fold increase in the fraction of gp350-positive cells over NaB treatment alone (Fig. 2D). As expected, treatment with AG490 resulted in lower intracellular levels of STAT3 (Fig. 2E). Thus, suppression of STAT3 function increases susceptibility to known lytic stimuli.

Inhibition of STAT3 function is sufficient for EBV lytic activation. Next, we investigated if the suppression of STAT3 function is adequate to induce lytic activation. When BL cells were treated with AG490, an increase in the fraction of lytically infected cells over vehicle-treated cells was observed (Fig. 3A). WP1066, a more potent analog of AG490, demonstrated a further increase in lytic activation. Concurrent increases in transcript levels from the lytic genes *BZLF1*, *BMRF1*, and *BFRF3* were also observed following treatment with WP1066 compared to the vehicle control (Fig. 3B). These observations suggested that interference with STAT3 function may be sufficient to induce lytic activation in BL cells. To determine if this observation extended to non-BL cells, we generated EBV-positive lymphoblastoid cell lines (EBV-LCL) from B cells of healthy subjects and patients with autosomal dominant hyper-IgE syndrome (AD-HIES or Job's syndrome). AD-HIES patients have a heterozygous dominant negative mutation in their *STAT3* gene that limits the amount of functional STAT3 without affecting the levels of total STAT3 (18, 27). Therefore, EBV-LCL derived from *in vitro* infection of B cells from AD-HIES patients (AD-HIES EBV-LCL) provide independent, genetically distinct functional knockdowns of STAT3. We enumerated the fraction of EA-D-expressing cells in AD-HIES and healthy LCL in the presence of AG490 or Stattic compared to vehicle control (Fig. 3C and D). Stattic irreversibly suppresses STAT3 by inhibiting its

dimerization and activation (20). We observed a statistically significant increase in the percentage of EA-D$^+$ cells in 36-h AG490-treated AD-HIES EBV-LCL compared to either AG490-treated healthy EBV-LCL or vehicle-treated AD-HIES EBV-LCL (Fig. 3C). Similar significant increases in the fractions of EA-D$^+$ cells in AD-HIES EBV-LCL were observed following 1 h of Stattic treatment (Fig. 3D). Additionally, compared to healthy donor-derived LCL treated with AG490, there was a statistically significant increase in the relative abundance of *BZLF1*, *BMRF1*, and *BFRF3* transcripts in AD-HIES LCL treated with AG490 (Fig. 3E). However, while immunoblot analyses also showed increases in EA-D and sVCA (small viral capsid antigen, a late lytic protein) protein levels in AG490-treated LCL derived from two AD-HIES patients with different mutations in the *STAT3* DNA-binding domain, the levels of ZEBRA remained relatively unchanged before and after AG490 treatment in both representative cell lines (Fig. 3F). ZEBRA, the master switch for latency to lytic transition, is temporally the earliest EBV lytic protein to be expressed. ZEBRA transcriptionally activates *BMRF1*, which encodes EA-D (28); expression of late proteins, such as sVCA, follows thereafter. Thus, the suppression of STAT3 function alone in AD-HIES LCL is sufficient to increase the number of lytically infected cells. This is noteworthy since LCL are typically resistant to known EBV lytic cycle-inducing signals.

While there was a trend toward increased lytic activation in AD-HIES LCL compared to healthy donor-derived LCL at baseline (Fig. 3C), the difference was not statistically significant. We postulated that this lack of a significant difference may be because EBV-LCL had accumulated unforeseen genetic changes from culturing for different lengths of time. We therefore infected B cells from three AD-HIES patients and three healthy donors with EBV at the same time. AD-HIES EBV-LCL showed significantly high basal levels of spontaneous lytic activation beginning at week 7 compared to EBV-LCL derived from healthy donors, demonstrating that cells with genetically suppressed levels of functional STAT3 are more susceptible to spontaneous EBV lytic activation (Fig. 3G).

Modulation of STAT3 levels functions as a host lytic switch. To further validate our findings, we transfected BL (HH514-16) cells with siRNA directed against *STAT3* and then treated cells with NaB at 24 h and enumerated lytically infected cells after another 48 h. This approach allowed us to eliminate potential off-target effects of JAK inhibitors. Compared to cells transfected with scrambled siRNA, transfection with siRNA to *STAT3* resulted in a reduction in the percentage of cells expressing high levels of STAT3 (−7.9% ± 2.17%), with a concurrent increase in the percentage of lytic cells (7.8% ± 2.03%) (Fig. 4A). There was also a statistically significant decrease in the relative abundance of *STAT3* transcript in cells transfected with siRNA to *STAT3* compared to those transfected with scrambled siRNA (Fig. 4B).

We reasoned that since lower levels of STAT3 promote susceptibility to lytic cycle-inducing agents, higher levels of functional STAT3 may favor a refractory state. HH514-16 cells were transfected with a cytomegalovirus (CMV) promoter-driven *STAT3* expression vector or an empty vector and then treated with NaB at 24 h and examined after another 48 h. Compared to cells transfected with the empty vector, transfection with a *STAT3* expression vector resulted in an increase in the percentage of cells expressing high levels of STAT3 (12.1% ± 1.43%), with a concurrent fall in the percentage of lytic cells (−7.7% ± 2.12%).

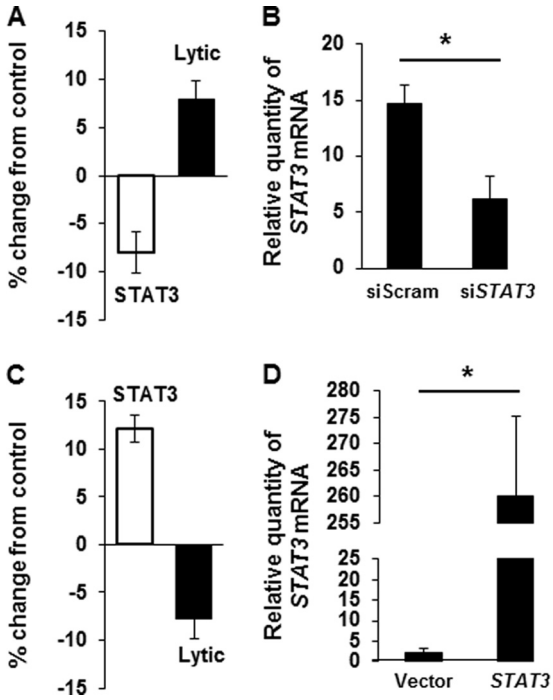

FIG 4 Levels of STAT3 regulate susceptibility to lytic activation in Burkitt lymphoma cells. (A and C) HH514-16 cells were transfected with either siRNA to *STAT3* (A) or the *STAT3* expression vector (C), treated with NaB 24 h later, and harvested after another 48 h. Changes in the percentage of cells expressing high levels of STAT3 (open bars) following transfection with *STAT3* siRNA (A) or the *STAT3* expression vector (C) compared to cells transfected with control scrambled siRNA (A) or the empty vector (C) are shown. Corresponding changes in the percentage of lytically infected cells (filled bars) were measured by flow cytometry using reference human sera. (B and D) Relative amounts of *STAT3* mRNA determined by qRT-PCR in transfected cells normalized to 18S rRNA levels by using the $\Delta\Delta C_T$ method. Cells were transfected with siRNA to *STAT3* or scrambled siRNA (B) and with the *STAT3* expression vector or the empty vector (D). Experiments were performed three times; means ± standard errors of the means are shown. *, $P < 0.05$ by one-way analysis of variance with *post hoc* Bonferroni analysis.

There was a statistically significant increase in the relative abundance of *STAT3* transcript in *STAT3*-transfected cells compared to empty vector-transfected cells (Fig. 4D). Transfection efficiencies of B-cell lines typically range from 10 to 15%. Thus, the intracellular level of STAT3 in EBV-infected cells influences susceptibility to lytic activation.

Expression profiling identifies transcriptional targets of STAT3 in refractory cells. Since STAT3, a well-known transcription factor, can transactivate several thousand genes, we examined the convergence of two genome-wide analysis measures: a publically available STAT3 chromatin immunoprecipitation-DNA sequencing (ChIP-seq) data set from EBV-LCL (GM12878) (29) and the Affymetrix HG-U133 Plus2.0 array probed by sorted refractory and lytic HH514-16 cells (NCBI GEO accession number GSE49568) that was used in the initial approach to identify STAT3 as a candidate of interest (11). We postulated that overlap between the two data sets would identify candidate genes that are involved in the STAT3-mediated regulation of lytic and refractory states. Probes with at least 2-fold increases in levels in lytic cells compared to refractory cells contributed to 1,345 genes (see Table S1 in the supplemental material), while 1,084 genes demonstrated in-

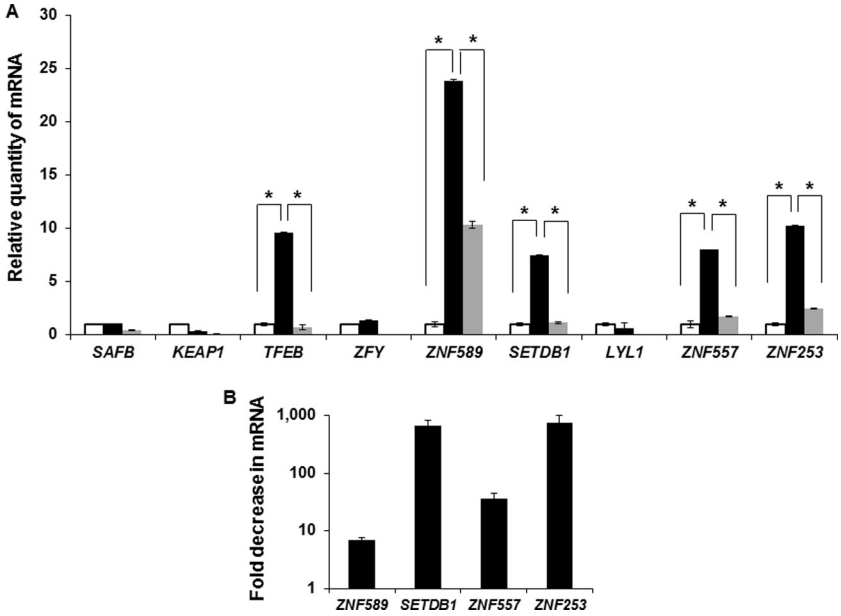

FIG 5 Elevated levels of KRAB-ZFP transcripts mark cells in the refractory/latent state. (A) Untreated but mock-sorted HH514-16 BL cells (open bars), NaB-treated sorted refractory cells (black bars), and NaB-treated sorted lytic cells (gray bars) were subjected to qRT-PCR using primers targeting nine candidate genes that are putative transcriptional targets of STAT3 and contribute to the "transcription" GO biological process pathway (see Table S6 in the supplemental material). Results represent means of relative amounts of RNA normalized to 18S rRNA levels ± standard errors of the means of three technical replicates from each of three independent sorting experiments. (B) LCL derived from 3 AD-HIES patients were exposed to AG490 (or vehicle control) for 36 h. Fold decreases in transcript levels of *ZNF589*, *SETDB1*, *ZNF557*, and *ZNF253* (three of these are KRAB-ZFPs) in AG490-exposed compared to vehicle-exposed cells are shown. Results represent means ± standard errors of the means.

creased transcript levels in refractory compared to lytic cells (see Table S2 in the supplemental material). Our analysis of the STAT3 ChIP-seq peak set of the EBV-positive LCL GM12878 produced a list of 8,276 STAT3-regulated genes. Out of 1,345 lytic genes, 381 overlapped 8,276 STAT3 targets (see Table S3 in the supplemental material), yielding a ratio of 28%. Out of 1,084 refractory genes, 641 overlapped STAT3 targets (see Table S4 in the supplemental material), yielding a ratio of 59%. With approximately 30,000 genes in the human genome, the global ratio of STAT3 target genes is 28%, suggesting that STAT3 targets were enriched within refractory cells. Although this finding was encouraging, the large number of potential STAT3 targets in refractory cells made the identification of STAT3-regulated candidate genes challenging. We therefore undertook an alternative approach in which we converted the lists of genes from the STAT3 ChIP-seq peak set and Affymetrix array data (see Tables S1 and S2 in the supplemental material) into Gene Ontology (GO) terms (30). Table S5 in the supplemental material shows concurrent GO terms between the STAT3 ChIP-seq data set and the Affymetrix data set of genes with increased or decreased levels of expression in the refractory compared to the lytic population (hypergeometric distribution, with a false discovery rate of <25% as the cutoff for each data set). This analysis identified only 26 concurrent ontologies from genes potentially regulated by STAT3 and from those that were expressed at higher levels within the refractory population ($P < 0.05$ by chi-square test). The lists of genes contributing to these 26 ontologies are presented in Table S6 in the supplemental material. Consistent with lower levels of STAT3 in lytic cells, no common terms were identified between the STAT3 ChIP-seq data set and the Affymetrix list of genes with increased levels of expression in lytic cells. Genes that contribute to this finite set of ontologies and are likely transcriptionally activated by STAT3 in refractory cells now represent new candidate players in the mechanisms by which STAT3 influences EBV lytic activation.

Refractory/latent cells show elevated levels of KRAB-ZFP transcripts. Of the top 20 candidate genes in Table S6 in the supplemental material, 12 contributed exclusively to the "transcription" biological pathway. For 9 of these genes, we successfully amplified cDNA from sorted lytic and sorted refractory HH514-16 BL cells and confirmed that transcript levels of 5 genes were significantly increased in refractory cells compared to lytic and untreated cells (Fig. 5A). Four of these genes, *ZNF589*, *SETDB1*, *ZNF557*, and *ZNF253*, contribute to the function of the KRAB-KAP1 transcriptional repressor, with 3 belonging to the family of KRAB-ZFPs. Transcript levels of all four genes were also suppressed after exposure of LCL from three AD-HIES patients to AG490 (Fig. 5B). KRAB-ZFPs are members of a superfamily of transcriptional repressors that bind DNA through their tandem zinc finger motifs and recruit histone deacetylases, histone methyltransferases (such as SETDB1), and heterochromatin proteins via their KRAB domains to mediate gene silencing (31). Thus, we have experimentally confirmed increased expression levels of three KRAB-ZFPs and a histone methyltransferase among the top candidate genes likely to be transcriptionally upregulated by STAT3 in refractory cells.

DISCUSSION

In this study, we provide evidence for a functional link between STAT3 and EBV lytic activation. Using approaches that examine gene expression within single cells, we demonstrate that modulation of intracellular levels of STAT3 affects the ability of EBV-infected B cells to respond to known lytic cycle-inducing stimuli.

By suppressing STAT3 function, latently infected B-cell lines can be made more permissive to lytic cycle-inducing agents. Moreover, suppression of STAT3 function increases spontaneous lytic activation in AD-HIES LCL. In contrast, overexpression of STAT3 results in maintenance of the refractory/latency state. The latter finding is consistent with the observation that STAT3, a transcription factor, is constitutively active in EBV tumors exhibiting viral latency (32, 33). Importantly, the link between STAT3 and resistance of EBV-infected B cells to viral lytic activation was confirmed in EBV-infected B cells from the blood of patients with primary EBV infection. Taken together, our findings implicate STAT3 in the partial permissiveness of B cells to EBV lytic activation and suggest that EBV may exploit the prosurvival and proproliferative host protein STAT3 for limiting lytic viral activation via recruitment of a powerful transcription repressor system.

EBV lytic replication is known to occur in the oropharyngeal compartment during IM. However, the existence of lytically infected B cells in peripheral blood has been questioned (34–36). In contrast to our findings, a previous study was unable to detect lytic replication in peripheral B cells (36). In our experiments, detection of lytically infected cells relied on the simultaneous recognition of multiple lytic antigens by high-titer antibodies in well-characterized EBV-positive sera (9, 11, 23). In comparison, that previous study was restricted to the detection of *BZLF1* transcripts, which may be expressed transiently or at low levels. Another reason for this difference in outcomes may be related to the timing of recruitment of IM patients. While our patients had evidence of seroconversion to EBV, they did not have evidence of atypical lymphocytes in peripheral blood. Atypical lymphocytes are indicative of cytotoxic T lymphocytes that rapidly remove lytically infected B cells from circulation as patients become symptomatic during IM (37). Patients in our study were very mildly symptomatic and were identified early in infection quite by chance by diagnostic testing. These factors resulted in the identification of lytically infected B cells in the blood during primary EBV infection.

While suppression of STAT3 function resulted in an expected increase in levels of the *BZLF1* transcript, we were surprised to find that considerable levels of ZEBRA existed at baseline in AD-HIES-derived LCL; however, progression of the lytic cycle occurred preferentially after treatment with AG490. Thus, while STAT3 may regulate *BZLF1* transcription, an additional level of control by STAT3, and potentially other host genes, may be exerted downstream of the expression of ZEBRA. High levels of ZEBRA at baseline in AD-HIES-derived LCL are likely due to lower baseline levels of functional STAT3 in these cells. Whether progression of the lytic cycle after treatment with AG490 occurs in cells already expressing ZEBRA at baseline or in cells newly expressing ZEBRA is presently unclear.

STAT3 transcriptionally regulates a broad range of cellular genes with diverse functions (12). Among viral genes, STAT3 activates LMP1 (32, 38), a latency protein that has been shown to block the induction of the lytic cycle (39). Our previous studies suggest that maintenance of the refractory state is not due to high levels of LMP1 expression in refractory cells (11). To determine how STAT3 may influence EBV lytic activation, we utilized two powerful resources to identify a finite group of STAT3 target genes in refractory cells. Confirmation of increased transcript levels of three KRAB-ZFPs and a histone methyltransferase during the refractory/latent state implicates STAT3-mediated recruitment of the KRAB-KAP1 repression system in curbing EBV lytic gene expression. Two of these, SETDB1 and ZNF589, have been shown to functionally interact with KAP1 to suppress transcription from targeted euchromatic regions of the genome (31, 40).

Patients with AD-HIES have been instrumental in uncovering the role of STAT3 in the development of cellular immune responses (16, 41, 42). With these patients, we were able to explore the influence of STAT3 on the life cycle of a globally relevant, persistent virus in humans. We also anticipate that mutations in AD-HIES patients will be invaluable in designing STAT3 mutants to address mechanistic questions related to EBV lytic activation. A recent study implicated STAT3 in varicella-zoster virus-mediated infection of human xenografts in mice (43). Another study found higher EBV loads in peripheral blood and impaired central memory T-cell responses in AD-HIES patients (42). Our findings suggest that the increased EBV load in such patients is likely due to a combination of enhanced lytic activation and persistence of such lytically infected B cells as a consequence of impaired EBV-directed T-cell responses.

STAT3 has been found to be constitutively active in EBV-positive tumors (32, 33). The discovery of a causal link between STAT3 and lytic susceptibility is consistent with the notion that active STAT3, leading to high levels of intracellular STAT3, may favor persistence of tumor cells by limiting lytic activation in EBV tumors. Whether STAT3 serves as a sensor for EBV to determine if the environment is conducive to lytic replication or maintenance of viral persistence through latency or whether EBV uses STAT3 as a cellular switch to promote lytic viral replication or maintain persistence remains to be determined. An understanding of how EBV manipulates host proteins such as STAT3 to regulate the flux between lytic and refractory cells will result in a better understanding of the pathogenesis of EBV-related diseases. We also expect that modulation of intracellular STAT3 as a means to control EBV lytic activation will have translational consequences for overcoming lethal EBV lymphomas. Such therapy may be extended to non-B-cell tumors as the contribution of EBV to such cancers continues to be unveiled (44).

ACKNOWLEDGMENTS

This study was supported by grants K08 AI062732, K12 HD001401, and 1UL1RR024139-02 and funds from The Research Foundation for The State University of New York to S.B.-M and from the National Health and Medical Research Council of Australia and the New South Wales Cancer Council to S.G.T.

We thank Steven Holland at the NIAID for providing access to AD-HIES patient samples, AD-HIES patients and healthy subjects at the NIH Primary Immune Deficiency Clinic for their participation, Nancy Reich for the use of pCMV-*STAT3* and control plasmids, and the Snyder laboratory at Stanford University for providing access to LCL ChIP-seq data via the ENCODE TFBS file database at UCSC's Genome Browser.

E.R.H., S.K., and S.B.-M. designed the study; E.R.H., S.K., and C.M. carried out the experiments; J.Z. performed bioinformatics analyses; A.F.F., U.P., and S.G.T. provided materials from patients and cell lines; P.J.F. provided the BZ1 antibody; E.R.H., S.K., and S.B.-M. analyzed data and interpreted the findings; and E.R.H. and S.B.-M. wrote the manuscript.

We have no conflicts of interest to disclose.

REFERENCES

1. **Tselis AC, Jenson HB.** 2006. Epstein-Barr virus. Taylor & Francis, New York, NY.
2. **Hong GK, Gulley ML, Feng WH, Delecluse HJ, Holley-Guthrie E,**

Kenney SC. 2005. Epstein-Barr virus lytic infection contributes to lymphoproliferative disease in a SCID mouse model. J. Virol. **79:**13993–14003.
3. **Mueller N, Evans A, Harris NL, Comstock GW, Jellum E, Magnus K, Orentreich N, Polk BF, Vogelman J.** 1989. Hodgkin's disease and Epstein-Barr virus. Altered antibody pattern before diagnosis. N. Engl. J. Med. **320:**689–695.
4. **Pallesen G, Sandvej K, Hamilton-Dutoit SJ, Rowe M, Young LS.** 1991. Activation of Epstein-Barr virus replication in Hodgkin and Reed-Sternberg cells. Blood **78:**1162–1165.
5. **van Esser JW, van der Holt B, Meijer E, Niesters HG, Trenschel R, Thijsen SF, van Loon AM, Frassoni F, Bacigalupo A, Schaefer UW, Osterhaus AD, Gratama JW, Lowenberg B, Verdonck LF, Cornelissen JJ.** 2001. Epstein-Barr virus (EBV) reactivation is a frequent event after allogeneic stem cell transplantation (SCT) and quantitatively predicts EBV-lymphoproliferative disease following T-cell-depleted SCT. Blood **98:**972–978.
6. **Feng WH, Israel B, Raab-Traub N, Busson P, Kenney SC.** 2002. Chemotherapy induces lytic EBV replication and confers ganciclovir susceptibility to EBV-positive epithelial cell tumors. Cancer Res. **62:**1920–1926.
7. **Fu DX, Tanhehco Y, Chen J, Foss CA, Fox JJ, Chong JM, Hobbs RF, Fukayama M, Sgouros G, Kowalski J, Pomper MG, Ambinder RF.** 2008. Bortezomib-induced enzyme-targeted radiation therapy in herpesvirus-associated tumors. Nat. Med. **14:**1118–1122.
8. **Perrine SP, Hermine O, Small T, Suarez F, O'Reilly R, Boulad F, Fingeroth J, Askin M, Levy A, Mentzer SJ, Di Nicola M, Gianni AM, Klein C, Horwitz S, Faller DV.** 2007. A phase 1/2 trial of arginine butyrate and ganciclovir in patients with Epstein-Barr virus-associated lymphoid malignancies. Blood **109:**2571–2578.
9. **Bhaduri-McIntosh S, Miller G.** 2006. Cells lytically infected with Epstein-Barr virus are detected and separable by immunoglobulins from EBV-seropositive individuals. J. Virol. Methods **137:**103–114.
10. **Gradoville L, Kwa D, El-Guindy A, Miller G.** 2002. Protein kinase C-independent activation of the Epstein-Barr virus lytic cycle. J. Virol. **76:**5612–5626.
11. **Daigle D, Megyola C, El-Guindy A, Gradoville L, Tuck D, Miller G, Bhaduri-McIntosh S.** 2010. Upregulation of STAT3 marks Burkitt lymphoma cells refractory to Epstein-Barr virus lytic cycle induction by HDAC inhibitors. J. Virol. **84:**993–1004.
12. **Yu H, Kortylewski M, Pardoll D.** 2007. Crosstalk between cancer and immune cells: role of STAT3 in the tumour microenvironment. Nat. Rev. Immunol. **7:**41–51.
13. **Frank DA.** 2007. STAT3 as a central mediator of neoplastic cellular transformation. Cancer Lett. **251:**199–210.
14. **Darnell JE, Jr.** 2002. Transcription factors as targets for cancer therapy. Nat. Rev. Cancer **2:**740–749.
15. **Hui-Yuen J, McAllister S, Koganti S, Hill E, Bhaduri-McIntosh S.** 2011. Establishment of Epstein-Barr virus growth-transformed lymphoblastoid cell lines. J. Vis. Exp. **2011:**3321. doi:10.3791/3321.
16. **Avery DT, Deenick EK, Ma CS, Suryani S, Simpson N, Chew GY, Chan TD, Palendira U, Bustamante J, Boisson-Dupuis S, Choo S, Bleasel KE, Peake J, King C, French MA, Engelhard D, Al-Hajjar S, Al-Muhsen S, Magdorf K, Roesler J, Arkwright PD, Hissaria P, Riminton DS, Wong M, Brink R, Fulcher DA, Casanova JL, Cook MC, Tangye SG.** 2010. B cell-intrinsic signaling through IL-21 receptor and STAT3 is required for establishing long-lived antibody responses in humans. J. Exp. Med. **207:**155–171.
17. **Ma CS, Chew GY, Simpson N, Priyadarshi A, Wong M, Grimbacher B, Fulcher DA, Tangye SG, Cook MC.** 2008. Deficiency of Th17 cells in hyper IgE syndrome due to mutations in STAT3. J. Exp. Med. **205:**1551–1557.
18. **Holland SM, DeLeo FR, Elloumi HZ, Hsu AP, Uzel G, Brodsky N, Freeman AF, Demidowich A, Davis J, Turner ML, Anderson VL, Darnell DN, Welch PA, Kuhns DB, Frucht DM, Malech HL, Gallin JI, Kobayashi SD, Whitney AR, Voyich JM, Musser JM, Woellner C, Schaffer AA, Puck JM, Grimbacher B.** 2007. STAT3 mutations in the hyper-IgE syndrome. N. Engl. J. Med. **357:**1608–1619.
19. **Rabson M, Heston L, Miller G.** 1983. Identification of a rare Epstein-Barr virus variant that enhances early antigen expression in Raji cells. Proc. Natl. Acad. Sci. U. S. A. **80:**2762–2766.
20. **Schust J, Sperl B, Hollis A, Mayer TU, Berg T.** 2006. Stattic: a small-molecule inhibitor of STAT3 activation and dimerization. Chem. Biol. **13:**1235–1242.
21. **Tung CP, Chang FR, Wu YC, Chuang DW, Hunyadi A, Liu ST.** 2011. Inhibition of the Epstein-Barr virus lytic cycle by protoapigenone. J. Gen. Virol. **92:**1760–1768.
22. **Batisse J, Manet E, Middeldorp J, Sergeant A, Gruffat H.** 2005. Epstein-Barr virus mRNA export factor EB2 is essential for intranuclear capsid assembly and production of gp350. J. Virol. **79:**14102–14111.
23. **Bhaduri-McIntosh S, Landry ML, Nikiforow S, Rotenberg M, El-Guindy A, Miller G.** 2007. Serum IgA antibodies to Epstein-Barr virus (EBV) early lytic antigens are present in primary EBV infection. J. Infect. Dis. **195:**483–492.
24. **Meydan N, Grunberger T, Dadi H, Shahar M, Arpaia E, Lapidot Z, Leeder JS, Freedman M, Cohen A, Gazit A, Levitzki A, Roifman CM.** 1996. Inhibition of acute lymphoblastic leukaemia by a Jak-2 inhibitor. Nature **379:**645–648.
25. **Yang J, Chatterjee-Kishore M, Staugaitis SM, Nguyen H, Schlessinger K, Levy DE, Stark GR.** 2005. Novel roles of unphosphorylated STAT3 in oncogenesis and transcriptional regulation. Cancer Res. **65:**939–947.
26. **Countryman JK, Gradoville L, Miller G.** 2008. Histone hyperacetylation occurs on promoters of lytic cycle regulatory genes in Epstein-Barr virus-infected cell lines which are refractory to disruption of latency by histone deacetylase inhibitors. J. Virol. **82:**4706–4719.
27. **Minegishi Y, Saito M, Tsuchiya S, Tsuge I, Takada H, Hara T, Kawamura N, Ariga T, Pasic S, Stojkovic O, Metin A, Karasuyama H.** 2007. Dominant-negative mutations in the DNA-binding domain of STAT3 cause hyper-IgE syndrome. Nature **448:**1058–1062.
28. **El-Guindy A, Heston L, Miller G.** 2010. A subset of replication proteins enhances origin recognition and lytic replication by the Epstein-Barr virus ZEBRA protein. PLoS Pathog. **6:**e1001054. doi:10.1371/journal.ppat.1001054.
29. **ENCODE Project Consortium.** 2011. A user's guide to the encyclopedia of DNA elements (ENCODE). PLoS Biol. **9:**e1001046. doi:10.1371/journal.pbio.1001046.
30. **Huang DW, Sherman BT, Lempicki RA.** 2009. Systematic and integrative analysis of large gene lists using DAVID bioinformatics resources. Nat. Protoc. **4:**44–57.
31. **Schultz DC, Ayyanathan K, Negorev D, Maul GG, Rauscher FJ, III.** 2002. SETDB1: a novel KAP-1-associated histone H3,lysine 9-specific methyltransferase that contributes to HP1-mediated silencing of euchromatic genes by KRAB zinc-finger proteins. Genes Dev. **16**(8):919–932.
32. **Chen H, Lee JM, Zong Y, Borowitz M, Ng MH, Ambinder RF, Hayward SD.** 2001. Linkage between STAT regulation and Epstein-Barr virus gene expression in tumors. J. Virol. **75:**2929–2937.
33. **Nepomuceno RR, Balatoni CE, Natkunam Y, Snow AL, Krams SM, Martinez OM.** 2003. Rapamycin inhibits the interleukin 10 signal transduction pathway and the growth of Epstein Barr virus B-cell lymphomas. Cancer Res. **63:**4472–4480.
34. **Prang NS, Hornef MW, Jager M, Wagner HJ, Wolf H, Schwarzmann FM.** 1997. Lytic replication of Epstein-Barr virus in the peripheral blood: analysis of viral gene expression in B lymphocytes during infectious mononucleosis and in the normal carrier state. Blood **89:**1665–1677.
35. **Al Tabaa Y, Tuaillon E, Jeziorski E, Ouedraogo DE, Bollore K, Rubbo PA, Foulongne V, Rodiere M, Vendrell JP.** 2011. B-cell polyclonal activation and Epstein-Barr viral abortive lytic cycle are two key features in acute infectious mononucleosis. J. Clin. Virol. **52:**33–37.
36. **Hochberg D, Souza T, Catalina M, Sullivan JL, Luzuriaga K, Thorley-Lawson DA.** 2004. Acute infection with Epstein-Barr virus targets and overwhelms the peripheral memory B-cell compartment with resting, latently infected cells. J. Virol. **78:**5194–5204.
37. **Hislop AD, Annels NE, Gudgeon NH, Leese AM, Rickinson AB.** 2002. Epitope-specific evolution of human CD8(+) T cell responses from primary to persistent phases of Epstein-Barr virus infection. J. Exp. Med. **195:**893–905.
38. **Chen H, Hutt-Fletcher L, Cao L, Hayward SD.** 2003. A positive autoregulatory loop of LMP1 expression and STAT activation in epithelial cells latently infected with Epstein-Barr virus. J. Virol. **77:**4139–4148.
39. **Prince S, Keating S, Fielding C, Brennan P, Floettmann E, Rowe M.** 2003. Latent membrane protein 1 inhibits Epstein-Barr virus lytic cycle induction and progress via different mechanisms. J. Virol. **77:**5000–5007.
40. **Peng H, Zheng L, Lee WH, Rux JJ, Rauscher FJ, III.** 2002. A common DNA-binding site for SZF1 and the BRCA1-associated zinc finger protein, ZBRK1. Cancer Res. **62:**3773–3781.
41. **Tangye SG, Cook MC, Fulcher DA.** 2009. Insights into the role of STAT3

in human lymphocyte differentiation as revealed by the hyper-IgE syndrome. J. Immunol. **182:**21–28.
42. **Siegel AM, Heimall J, Freeman AF, Hsu AP, Brittain E, Brenchley JM, Douek DC, Fahle GH, Cohen JI, Holland SM, Milner JD.** 2011. A critical role for STAT3 transcription factor signaling in the development and maintenance of human T cell memory. Immunity **35:**806–818.
43. **Sen N, Che X, Rajamani J, Zerboni L, Sung P, Ptacek J, Arvin AM.** 2012. Signal transducer and activator of transcription 3 (STAT3) and survivin induction by varicella-zoster virus promote replication and skin pathogenesis. Proc. Natl. Acad. Sci. U. S. A. **109:**600–605.
44. **Amarante MK, Watanabe MA.** 2009. The possible involvement of virus in breast cancer. J. Cancer Res. Clin. Oncol. **135:**329–337.

Journal of Virology

Signal Transducer and Activator of Transcription 3 Limits Epstein-Barr Virus Lytic Activation in B Lymphocytes

Erik R. Hill, Siva Koganti, Jizu Zhi, Cynthia Megyola, Alexandra F. Freeman, Umaimainthan Palendira, Stuart G. Tangye, Paul J. Farrell and Sumita Bhaduri-McIntosh

J. Virol. **2013, 87(21):11438. DOI: 10.1128/JVI.01762-13. Published Ahead of Print 21 August 2013.**